Estimating best fit binary mixing lines in the Day plot

David Heslop[1] and Andrew P. Roberts[1]

Received 16 August 2011; revised 2 November 2011; accepted 7 November 2011; published 19 January 2012.

[1] The Day plot is employed commonly to make inferences concerning the mean domain state of magnetic mineral assemblages. In recent years the concept of the Day plot as a representation of a two-part (binary) mixing space has gained popularity, with data sets being compared to theoretical curves that represent combinations of particles with different domain states. Our understanding of the behavior of mixtures within the Day plot, however, remains limited, and little progress has been made in terms of quantitative statistical analysis. We present an approach, based on linear mixing theory, with which a data-optimized binary mixing line can be found for a collection of hysteresis loops and their corresponding backfield demagnetization curves. The empirical best fit mixing line can then be used to determine a trend through the Day plot. Such trend lines help to constrain interpretation of rock magnetic data and aid in identification of binary mixtures. In cases where the trend line does not provide a good fit to the data, it can be concluded that the examined samples do not originate from a two-part linear mixing. The proposed method is demonstrated using both numerical simulations and geological data sets.

Citation: Heslop, D., and A. P. Roberts (2012), Estimating best fit binary mixing lines in the Day plot, *J. Geophys. Res.*, *117*, B01101, doi:10.1029/2011JB008787.

1. Introduction

[2] Since its introduction over 30 years ago, the Day plot [*Day et al.*, 1977] has become a widely used tool with which to infer the mean domain state of a magnetic mineral assemblage. The coordinates of the Day plot are the ratios of the saturation remanent magnetization to the saturation magnetization (M_{rs}/M_s) and the coercivity of remanence to the coercivity (B_{cr}/B_c), which can be determined from a major hysteresis loop and a direct current demagnetization (DCD) curve. The Day plot is typically demarcated into different zones that are indicative of single domain (SD), pseudosingle domain (PSD) and multidomain (MD) behavior on the basis of both theoretical and empirical arguments. It is thus a simple task to determine the M_{rs}/M_s and B_{cr}/B_c ratios for a given sample and to assign a mean domain state according to the boundaries defined for the Day plot [*Day et al.*, 1977].

[3] In recent years, representation of magnetic assemblages in the Day plot has come under close scrutiny. For example, *Roberts et al.* [1995a], *Tauxe et al.* [1996], *Carter-Stiglitz et al.* [2001], and *Dunlop* [2002a] showed how mixing two magnetic assemblages with different domain states could produce a variety of magnetization and coercivity ratios depending on the mixing proportions. The classic example of such an effect is the mixture of SD and MD particles that lie commonly in the PSD field even though the concentration of PSD grains could be zero [*Dunlop*, 2002a]. *Sprowl* [1990] and *Muxworthy et al.* [2003] showed that magnetostatic interactions can strongly influence the position of SD particles in the Day plot. Specifically, magnetization and coercivity ratios indicative of MD grains can be produced by assemblages of strongly interacting SD particles. *Lanci and Kent* [2003] and *Heslop* [2005] investigated the role of thermal activation in the Day plot and demonstrated that trends across the diagram from the SD to MD fields could be produced by introducing thermal energy into the magnetic system.

[4] The variety of processes that can influence the behavior of magnetic particles demonstrates the difficulty in interpreting the meaning of a data point for a single sample within the Day plot. *Tauxe et al.* [1996] argued that any given location in the Day plot could correspond to an infinite number of loop shapes, therefore hysteresis ratios are a completely nonunique descriptor. More advanced hysteresis techniques, such as first-order reversal curve diagrams [*Pike et al.*, 1999; *Roberts et al.*, 2000], have been developed to quantify magnetic assemblages and to reduce inherent ambiguities in interpretation of Day plots. However, the Day plot is still valuable for discriminating variability in magnetic mineral assemblages if this ambiguity can be constrained.

[5] Forward modeling of magnetic mixtures in the Day plot by *Dunlop* [2002a, 2002b] has facilitated interpretation of two-part mixtures. The library of binary mixing lines presented by *Dunlop* [2002a] has been used widely to make inferences concerning the composition of samples according to their position within the Day plot. These binary mixing models cannot, however, be optimized to a given data set. Additionally, such forward models do not allow testing of the appropriateness of a binary mixing system to provide an adequate model of a data set. Finally, given that points in the

[1]Research School of Earth Sciences, Australian National University, Canberra, ACT, Australia.

0148-0227/12/2011JB008787

Day plot are nonunique, it is not possible to attribute a sample to a binary mixing system solely on the basis of it lying in close proximity to a forward model line. Instead, identification of a binary mixing system must be made on the basis of a collection of samples that describe a physically realistic trend within the diagram.

[6] Attempts to quantify data-optimized trends through the Day plot have focused on estimating power laws that provide a best fit to M_{rs}/M_s versus B_{cr}/B_c data [*Parry*, 1982; *Jackson*, 1990; *Channell and McCabe*, 1994; *Gee and Kent*, 1995; *Roberts*, 1995; *Suk and Halgedahl*, 1996; *Roberts et al.*, 2011]. A number of the theoretical binary mixing lines calculated by *Dunlop* [2002a] and the experimental mixing lines of *Dunlop and Carter-Stiglitz* [2006], however, do not follow power laws. While power laws may provide a first-order approximation applicable to the types of trends sometimes observed in the Day plot, linear mixture theory provides a basis to calculate a best fit (i.e., data-optimized) line and associated goodness-of-fit statistics for binary mixtures.

[7] We demonstrate here how a best fit binary mixing line can be calculated for hysteresis data sets. Such best fit lines are useful because they can help to identify and quantify binary mixtures. Just as importantly, they can also reveal when a trend through the Day plot may not be due to binary mixing. While it is possible to consider more complex mixtures, for example ternary mixtures, such schemes cannot be described by single curves through the Day plot. For example, describing a collection of ternary mixtures would require a form similar to (but not exactly equal to) a hyperbolic triangle, which is a case that has received limited attention [e.g., *Lascu et al.* 2010]. We focus on binary mixtures in this paper and consider higher-order mixtures elsewhere (D. Heslop and A. P. Roberts, A method for unmixing magnetic hysteresis loops, submitted to *Journal of Geophysical Research*, 2011).

2. Calculation of a Best Fit Binary Mixing Line

[8] Linear mixing theory has been applied to a wide variety of problems in the geosciences [e.g., *Ehrlich and Full*, 1987]. In his forward modeling of binary mixtures in the Day plot, *Dunlop* [2002a] also adopted a linear mixing approach based upon the magnetic properties of two end-member compositions, referred to here as C and D, with volume fractions of f_C and f_D, respectively. To ensure physically realistic and conservative mixing, the volume fractions must also be constrained so that $f_C \geq 0$, $f_D \geq 0$ and $f_C + f_D = 1$. Under an assumption of linear mixing the magnetization, M, at a given field, B, is simply a linear combination of the two end-member magnetizations according to their volume fractions:

$$M(B) = f_C M_C(B) + f_D M_D(B). \quad (1)$$

As the volume fractions shift from $f_C = 1$ to $f_D = 1$, $M(B)$ will follow a straight path between $M_C(B)$ and $M_D(B)$, defining a binary mixing line. This general relationship holds for the case where multiple values of B are considered simultaneously, for example, the fields employed in a hysteresis measurement. In the case of p measured fields, the binary mixing scheme will be defined by a straight line passing through p-dimensional space between the points defined by C and D. In forward modeling experiments such as those of *Dunlop* [2002a], the positions of C and D are defined in advance and the mixing system can be quantified by sampling the line between the two end-members. For the vast majority of natural data sets the end-members are not known and instead an empirical mixing model must be formulated that is optimized to the available data.

[9] If linear mixing theory is to be applied to the Day plot it is necessary to assume that hysteresis loops and DCD curves of individual magnetic components are linearly additive. Experiments have demonstrated that such an assumption may be violated at high magnetic mineral concentrations because of magnetostatic interactions [*Roberts et al.*, 1995a; *Lees*, 1997; *Carter-Stiglitz et al.*, 2001; *Muxworthy et al.*, 2003]. Unfortunately, breakdown of linear additivity and its influence on the "unmixing" of magnetic measurements remains poorly understood. Thus, while an assumption of linear additivity is useful because it simplifies the unmixing strategy [*Carter-Stiglitz et al.*, 2001], it is important to consider that linearity may break down if magnetostatic interactions are significant between the different parts of the mixture.

[10] In the case of the Day plot, *Dunlop* [2002a] and *Dunlop and Carter-Stiglitz* [2006] showed that a collection of linear mixtures based on combining two fixed compositions, such as SD and MD particles, appear as curves within the Day plot that do not follow any obvious functional form. Estimation of a linear binary mixing model is therefore best tackled within the original (field versus magnetization) measurement space rather than within the Day plot.

[11] Consider a data set composed of hysteresis loops and their corresponding DCD curves measured over sequences of r_1 and r_2 common fields, respectively. As a first step the hysteresis loops must be corrected for any offsets and paramagnetic contributions [*Jackson and Solheid*, 2010]. Within the Day plot only the shape of the hysteresis data is important, i.e., the absolute values of the magnetizations are irrelevant, so as a first step each hysteresis loop can be normalized to $M_s = 1$. On the basis of this normalization, each DCD curve must have its initial value normalized to the M_{rs}/M_s value of its corresponding hysteresis loop. These normalizations make the data concentration independent, which ensures that the hysteresis loops and DCD curves are consistent with the assumption of fractional abundances upon which the linear mixing model discussed above is based.

[12] To visualize the mixing problem for a collection of samples, each individual sample is represented by r_1 hysteresis values and r_2 DCD values and thus can be thought of as a single point in a $(r_1 + r_2)$-dimensional coordinate system. The origin of the coordinate system will correspond to the centroid of the data set. As discussed above, in the case of an ideal binary mixing system all the sample points will lie along a straight line connecting the two end-members. For natural systems the end-members are typically unknown and the mixing line must be estimated from the data. The optimal binary mixing line to describe the data is obtained from the coordinates of the origin and the straight line through the $(r_1 + r_2)$-dimensional system that passes through the origin and that describes the maximum variance in the

data. This line of maximum variance can be found by eigenvector analysis [*Jolliffe*, 2002]. The point defined by the projection of any given sample onto this line of maximum variance then corresponds to its position within the binary mixing space. Any position along the fitted line can be transformed back into the measurement space, thereby producing an estimated hysteresis loop and DCD curve from which M_{rs}/M_s and B_{cr}/B_c can be obtained. It is important to note that the above approach defines the best fit line optimized to the data, but it does not define the specific model end-members responsible for the mixing. While in a perfect system it is known that the end-members are located on the line of maximum variance and must be more distant from the origin than any of the observed data points, their absolute position cannot be determined.

[13] The numerical strategy for obtaining the binary mixing trend line through the Day plot follows the steps outlined above for a large number of positions along the binary mixing line defined by eigenvector analysis. The sampled positions will describe a straight line in the mixing space, but will yield a curved trend within the Day plot. The procedure for calculating the trend line at a collection of discrete points is described below.

[14] The method of finding the line of maximum variance to characterize binary mixing systems is not limited to hysteresis and DCD data sets. The outlined approach can be applied to any set of measurements thought to exhibit linear additivity and originate from a two-part mixing scheme. Given the general nature of the approach, we define a binary mixture differently than *Dunlop* [2002a], who limited the cases considered to the mixing of different domain states of magnetite. The best fit approach is more relaxed and allows binary mixtures to be composed of any two magnetic components. This means that the components may themselves be mixtures that contain different magnetic domain states and mineralogic compositions. Interactions within the individual components are also permissable as long as the level of interaction does not change between the samples and there are no interactions between the two parts of the mixture. Thus, while *Dunlop* [2002a] considered mixing of discrete domain states, our best fit approach provides an empirical derivation of a mixing model resulting from two invariant components.

[15] In natural systems that undergo slight changes in the composition or level of interactions of the individual components through time there will be deviations from a perfect binary mixing model. Minor variability of this type will produce a scattering around the true mixing line and this must be taken into account during estimation of the best fit mixing line. Experimental noise will have a similar influence. Alternatively, more complex systems, i.e., those consisting of more than two components, cannot be approximated adequately by a binary mixing model and will produce spurious best fit lines in the Day plot. Identifying such complex systems is important when assessing the validity of a best fit binary mixing line.

[16] Consider a data matrix, $\boldsymbol{X_1}$, that contains the normalized (M_S = 1) hysteresis data and is constructed to have a size of $n \times r_1$, with one sample per row (for a total of n samples) and one set of magnetizations per column (for a total of r_1 fields). The inherent inversion symmetry of hysteresis loops makes it unnecessary to include full loops in $\boldsymbol{X_1}$. Instead the matrix can be formed from a collection of either lower or upper branches of the hysteresis loops. A second data matrix, $\boldsymbol{X_2}$, is constructed to contain the normalized DCD curves with a size $n \times r_2$, again with one sample per row (for a total of n samples) and one set of remanences per column (for a total of r_2 applied fields).

[17] To simplify processing, the hysteresis and DCD data matrices are *centered* in advance, i.e., the mean of each column in the two matrices is set to zero. Centering the data adjusts the origin of the multidimensional coordinate system discussed above to zero along each axis. A column centered version, $\boldsymbol{C}$, of a data matrix, for example, $\boldsymbol{X_1}$, can be formed by (in matrix notation):

$$\boldsymbol{C_1} = \boldsymbol{X_1} - \frac{\mathbf{1}_n \mathbf{1}_n^T \boldsymbol{X_1}}{n}, \tag{2}$$

where $\mathbf{1}_n$ is a column vector composed of n ones and ^{T} denotes a matrix transpose. Typically hysteresis loops contain many more measurement points than DCD curves, i.e., $r_1 \gg r_2$, which biases the best fit line toward providing a good approximation of $\boldsymbol{X_1}$ at the expense of $\boldsymbol{X_2}$. This implies that the two data matrices should be normalized in order that they carry approximately equal weight in the analysis. To achieve such a weighting each centered matrix is divided by its Frobenius norm. Using the matrix $\boldsymbol{C_1}$ as an example, the normalization yields:

$$\boldsymbol{W_1} = \frac{\boldsymbol{C_1}}{\sqrt{\mathrm{tr}(\boldsymbol{C_1}\boldsymbol{C_1}^T)}}, \tag{3}$$

where tr() represents the trace of the matrix. The combined normalized data matrices can now be factorized by singular value decomposition (SVD) [*Jolliffe*, 2002]:

$$\boldsymbol{U}\boldsymbol{S}\begin{bmatrix} \boldsymbol{V_1} \\ \boldsymbol{V_2} \end{bmatrix}^T = [\, \boldsymbol{W_1} \quad \boldsymbol{W_2} \,] = \boldsymbol{W}. \tag{4}$$

In this form the columns of $\boldsymbol{U}$ are the eigenvectors of $\boldsymbol{W}\boldsymbol{W}^{\boldsymbol{T}}$, the columns of $\boldsymbol{V}$ are the eigenvectors of $\boldsymbol{W}^T\boldsymbol{W}$ and the nonzero values along the diagonal of $\boldsymbol{S}$ are the square roots of the eigenvalues of both $\boldsymbol{W}\boldsymbol{W}^{\boldsymbol{T}}$ and $\boldsymbol{W}^T\boldsymbol{W}$.

[18] The first column of $\boldsymbol{V}$, denoted as $\boldsymbol{v}_{(*,\mathbf{1})}$, corresponds to the line of maximum variance through the centered $r_1 + r_2$ dimensional data cloud given by $\boldsymbol{W}$. The positions of the centered and weighted samples, i.e., the rows of $\boldsymbol{W}$, along the line of maximum variance are then given by $\boldsymbol{u}_{(*,\mathbf{1})}s_{(1,1)}$. In this way the values of $\boldsymbol{u}_{(*,\mathbf{1})}$ give an expression of the relative compositions of the samples with respect to the centered and weighted binary mixing space. The least squares approximation to $\boldsymbol{W}$, denoted as $\hat{\boldsymbol{W}}$, estimated from the binary mixing model is therefore given by:

$$\hat{\boldsymbol{W}} = \boldsymbol{u}_{(*,\mathbf{1})}s_{(1,1)}\begin{bmatrix} \boldsymbol{v}_{\mathbf{1}(*,\mathbf{1})} \\ \boldsymbol{v}_{\mathbf{2}(*,\mathbf{1})} \end{bmatrix}^T. \tag{5}$$

If the hysteresis loops and DCD curves are part of a linear binary mixing system the difference between $\boldsymbol{W}$ and $\hat{\boldsymbol{W}}$ can be attributed predominantly to measurement noise or minor deviations from a perfect mixing system (as outlined in

section 2). To measure the validity of a binary mixing model in describing the data, the proportion of the total variance of $\boldsymbol{W}$ that is described by the mixing model, i.e., $\hat{\boldsymbol{W}}$, can be found as:

$$L = \frac{\left[\frac{s_{(1,1)}}{\sqrt{n-1}}\right]^2}{\mathrm{tr}\left(\left[\frac{\boldsymbol{S}}{\sqrt{n-1}}\right]^2\right)}. \quad (6)$$

If $\hat{\boldsymbol{W}} = \boldsymbol{W}$, the hysteresis data can be described perfectly by the binary mixing model yielding $L = 1$. The reconstructed hysteresis matrix, $\hat{\boldsymbol{X}}_{\boldsymbol{1}}$, estimated from the binary mixing model is given by:

$$\hat{\boldsymbol{X}}_1 = \boldsymbol{u}_{(*,\boldsymbol{1})} s_{(1,1)} \boldsymbol{v}_{\boldsymbol{1}(*,\boldsymbol{1})}{}^T \sqrt{\mathrm{tr}(\boldsymbol{C_1 C_1}^T)} + \frac{\boldsymbol{1}_n \boldsymbol{1}_n^T \boldsymbol{X_1}}{n}, \quad (7)$$

which includes removing the normalization and centering from the least squares approximation. Similarly, the reconstructed DCD data matrix, $\hat{\boldsymbol{X}}_{\boldsymbol{2}}$, is given by:

$$\hat{\boldsymbol{X}}_{\boldsymbol{2}} = \boldsymbol{u}_{(*,\boldsymbol{1})} s_{(1,1)} \boldsymbol{v}_{\boldsymbol{2}(*,\boldsymbol{1})}{}^T \sqrt{\mathrm{tr}(\boldsymbol{C_2 C_2}^T)} + \frac{\boldsymbol{1}_n \boldsymbol{1}_n^T \boldsymbol{X_2}}{n}. \quad (8)$$

The best fit binary mixing line can be sampled at a point within the data distribution by selecting a value within the interval $[\min(\boldsymbol{u}_{(*,\boldsymbol{1})}), \max(\boldsymbol{u}_{(*,\boldsymbol{1})})]$ and then reconstructing the hysteresis loop and DCD curve corresponding to this point. For a newly selected value, u^p, it is possible to reconstruct the corresponding hysteresis branch, $\hat{\boldsymbol{x}}_{\boldsymbol{1}}^{\boldsymbol{p}}$, and DCD curve, $\hat{\boldsymbol{x}}_{\boldsymbol{2}}^{\boldsymbol{p}}$, as:

$$\hat{\boldsymbol{x}}_{\boldsymbol{1}}^{\boldsymbol{p}} = u^p s_{(1,1)} \boldsymbol{v}_{\boldsymbol{1}(*,\boldsymbol{1})}{}^T \sqrt{\mathrm{tr}(\boldsymbol{C_1 C_1}^T)} + \frac{\boldsymbol{1}_n^T \boldsymbol{X_1}}{n}, \quad (9)$$

$$\hat{\boldsymbol{x}}_{\boldsymbol{2}}^{\boldsymbol{p}} = u^p s_{(1,1)} \boldsymbol{v}_{\boldsymbol{2}(*,\boldsymbol{1})}{}^T \sqrt{\mathrm{tr}(\boldsymbol{C_2 C_2}^T)} + \frac{\boldsymbol{1}_n^T \boldsymbol{X_2}}{n}. \quad (10)$$

Once M_{rs}, M_s and B_c are established from $\hat{\boldsymbol{x}}_{\boldsymbol{1}}^{\boldsymbol{p}}$ and B_{cr} is determined from $\hat{\boldsymbol{x}}_{\boldsymbol{2}}^{\boldsymbol{p}}$, the location within the Day plot of the point corresponding to the position u^p on the mixing line can be found. If this procedure is repeated for numerous values of u^p, a discretely sampled representation of the best fit line can be obtained. It is also possible to extend the line beyond the range of the data by selecting a value of u^p outside the interval $[\min(\boldsymbol{u}_{(*,\boldsymbol{1})}), \max(\boldsymbol{u}_{(*,\boldsymbol{1})})]$. As with all trend line fitting and analysis, extreme caution must be exercised when extrapolating the line outside the measured data distribution.

[19] Finally, it is important to note that least squares methods such as SVD are vulnerable to outlying observations. This means that even if a small number of the measured hysteresis loops are outlying with respect to the binary mixing model of interest, for example, due to an ash layer within a sediment sequence, the determined mixing line may be affected adversely. There are two alterative approaches to reducing the influence of outliers on the calculated trend line. First, it is possible to use a multivariate statistical test to identify the loops that are outlying with respect to the robust covariance structure of $[\boldsymbol{X_1}\ \boldsymbol{X_2}]$ and then remove them from the analysis [*Rousseeuw and van Zomeren*, 1990]. Second, it is possible to employ a robust version of either principal component analysis [*Croux et al.*, 2007] or SVD [*Hawkins et al.*, 2001] to reduce the influence of the outliers on the estimated mixing line.

3. Testing the Validity of the Best Fit Mixing Line

[20] The described approach is designed specifically for binary mixtures. Thus, if it is applied to a more complex mixture or to a collection of samples that do not originate from a mixing system, it will yield spurious results. While the proportion of the variance described by the mixing line, defined by equation (6), provides a guide as to how well the data can be described, it does not provide conclusive evidence of a binary mixing model. To guard against the inappropriate assumption of a binary mixture, a bootstrap scheme can be used to test the fidelity of the derived mixing line.

[21] For each iteration of the bootstrap, n rows of $\boldsymbol{X_1}$ and their corresponding DCD curves from $\boldsymbol{X_2}$ were selected for analysis and placed in the matrices $\boldsymbol{X_1^{boot}}$ and $\boldsymbol{X_2^{boot}}$. This scheme was performed *with replacement*, thus it was possible for any given row to be selected more than once [*Efron and Tibshirani*, 1993]. The $[\boldsymbol{X_1^{boot}}\ \boldsymbol{X_2^{boot}}]$ binary mixing line and its associated value of L were then calculated. This process was repeated 1000 times and the resultant trend lines were plotted with the trend line obtained for the complete data set.

[22] The form of the bootstrap trend lines provides important information concerning the validity of the model and the possible presence of outliers. Scatter of the bootstrap lines may indicate small deviations from a perfect linear mixing system resulting from slight changes in the magnetic properties of samples that cannot be adequately represented by a binary mixing system. If the lines describe paths through the Day plot that appear to be unreasonable within the framework of our understanding of magnetic mixtures, it is feasible that the model has been applied inappropriately. This currently remains a subjective judgement; however, as will be shown in an example below, the information provides clear grounds for certain models to be rejected. Alternatively, if the paths of the bootstrap trend lines lack internal consistency, it may be indicative of the presence of outlying samples and a more robust analysis technique should be adopted.

4. Numerical Examples

[23] The following numerical examples demonstrate the proposed method for noise-free, linear mixtures. The first example is of a binary mixing system where the application of the proposed approach is appropriate. The second example illustrates the problems associated with attempting to represent a more complex ternary mixing system with a binary mixing line.

4.1. A Binary Mixture

[24] To demonstrate the described approach, a pair of hysteresis loops and their corresponding DCD curves were selected, with M_{rs}/M_s versus B_{cr}/B_c values similar to those expected for assemblages of SD and MD grains (Figure 1). Fifteen mixed hysteresis loops and DCD curves were then produced by combining the SD and MD curves in random

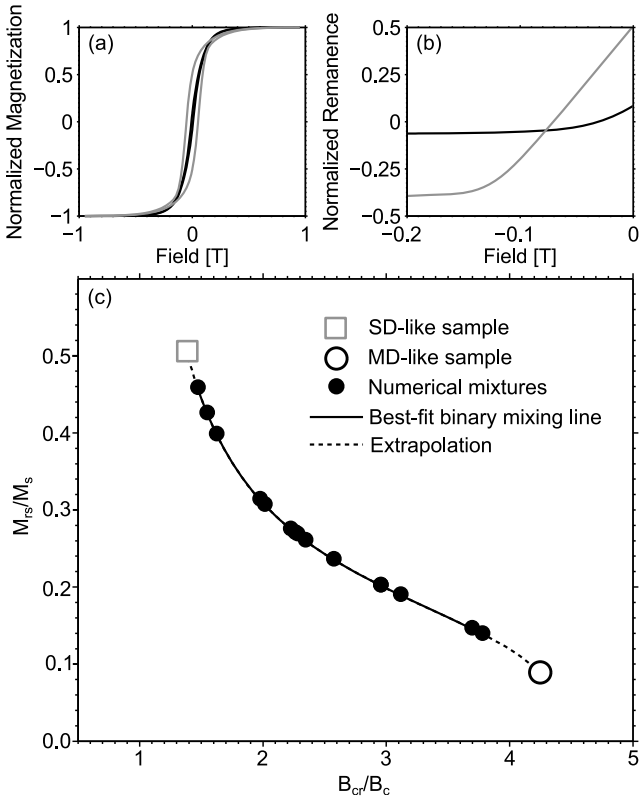

Figure 1. A numerical mixing experiment based on (a) hysteresis loops and (b) direct current demagnetization (DCD) curves for samples with SD-like (gray) and MD-like (black) magnetic properties. (c) Using the proposed approach, a trend line can be calculated on the basis of the best fit linear binary mixing model obtained from 15 numerical mixtures (solid symbols) of the SD-like and MD-like samples (open symbols). Within the Day plot, the binary mixing line (solid line) is curved and fits the data points perfectly. In this noise-free example it is also possible to extend the mixing line beyond the data distribution, providing a reliable extrapolation (dashed line) within the physically realistic region of the diagram.

relative proportions limited to the interval [0.05, 0.95]. By limiting the relative proportions to the specified interval, pure versions of the SD and MD curves are not included in the analysis, which provides a more geologically realistic example and allows extrapolation of the trend line to be demonstrated. The path of the data points through the Day plot follows a pattern similar to that described by *Dunlop and Carter-Stiglitz* [2006]. At high values of M_{rs}/M_s (low values of B_{cr}/B_c), the path defined by the data points has a concave-up form, while at low values of M_{rs}/M_s (high values of B_{cr}/B_c), it is concave-down.

[25] Using the approach described in section 2, a trend line composed of a large number of discrete points was calculated. In this case the data are composed of a noise-free linear binary mixing model, therefore the trend line fits the points in the Day plot perfectly (Figure 1c). In this noise-free example extrapolation outside of the data interval is reliable, with the mixing line eventually passing through the SD and MD points. In the presence of noise, however, extrapolation beyond the interval described by the data needs to be performed with extreme caution and should not be extended beyond the physically realistic regions of the diagram.

4.2. A Ternary Mixture

[26] A ternary mixing system was constructed with the SD and MD cases employed in the previous example and an additional high-coercivity hematite sample (Figures 2a and 2b). Addition of the third component means that the mixing system must be represented as a plane rather than as a line. Therefore, the ternary mixing system defines an area in the Day plot rather than a curve (Figure 2c). The best fit binary approximation to the ternary mixing space provides a poor representation of the true system. In the case of natural mixing systems, where the complexity of a given mixing scheme may be unknown, use of a binary approximation to a higher-order system could be spurious. This example demonstrates the dangers associated with approximating higher-order mixing systems with a binary scheme.

5. Geological Examples

[27] To demonstrate calculation of best fit binary mixing lines for real data, three examples are given based on

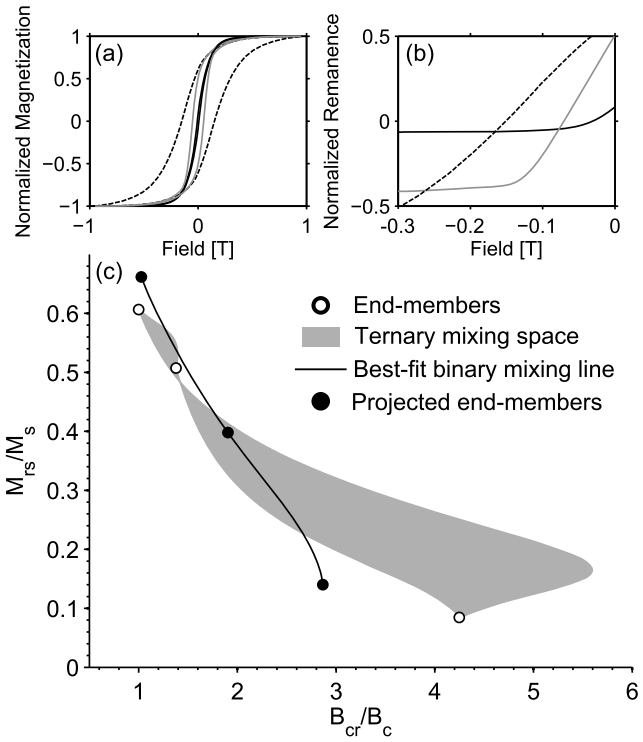

Figure 2. A numerical ternary mixing experiment based on (a) hysteresis loops and (b) DCD curves for SD-like (gray), MD-like (black), and high-coercivity (dashed lines) cases. (c) In the Day plot the three-component system defines a mixing space (shading) with vertices corresponding to the pure end-members (open symbols). The binary mixing line that provides the best fit approximation to the mixing space is shown as a solid line. The positions of the three end-members projected onto the binary mixing line are indicated by solid symbols.

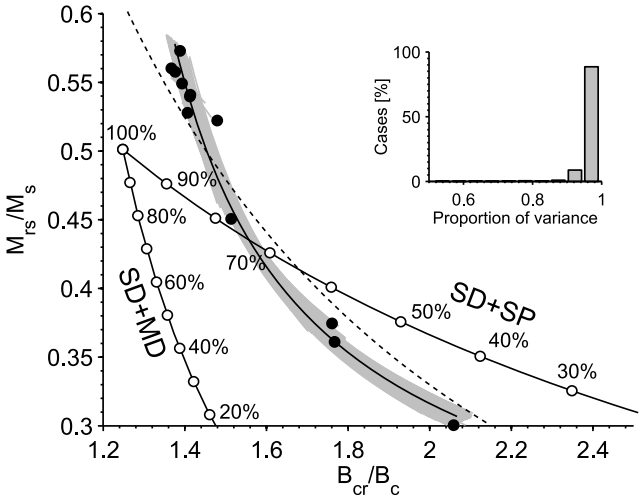

Figure 3. Best fit trend line (thick black line) and bootstrap trend lines (gray lines) for data from Plio-Pleistocene marine sediments exposed in Crostolo River, Italy (solid symbols, n = 12) [*Roberts et al.*, 2005]. The trend line has a form that is typical of the representation of binary mixing systems in the Day plot and, on the basis of a global data compilation of greigite-bearing samples, can be attributed to a SD + SP binary mixing system [*Roberts et al.*, 2011]. The magnetite SD + SP and SD + MD mixing lines of *Dunlop* [2002a] are shown for comparison (solid lines with percentage of SD indicated). Note the offset in maximum M_{rs}/M_s values between the magnetite models and the greigite data that results from the magnetocrystalline anisotropy of greigite. The best fit power law $M_{rs}/M_s = 0.81(B_{cr}/B_c)^{-1.3}$ obtained by *Roberts et al.* [2011] for a collection of 190 greigite samples is shown as a dashed line and is in better agreement with the best fit trend line than the magnetite models. The inset is a plot of the distribution of the proportional variance of each bootstrap line (i.e., the collection of L values from equation (6) for the ensemble of bootstraps).

published sample sets with well quantified magnetic assemblages. The first two data sets are thought to come from true binary mixing systems, while the third does not. This final case provides an example of a higher-order mixing system and demonstrates how the nonunique nature of the Day plot can lead to spurious interpretations if the assumption of binary mixing is not tested.

5.1. Crostolo River Section, Italy

[28] The magnetic assemblage within Plio-Pleistocene marine sediments from the Crostolo River section in Italy is dominated by authigenic greigite [*Tric et al.*, 1991; *Roberts et al.*, 2005]. The distribution of particle sizes that forms during authigenic sedimentary greigite growth typically ranges from SP to SD, which effectively forms a two-domain state mixing system [*Roberts*, 1995; *Roberts et al.*, 2011]. In a Day plot, data from the Crostolo River sediments describe a concave-up path (Figure 3), which is consistent with the expected form of SD + SP trends through the Day diagram [*Tauxe et al.*, 1996; *Dunlop*, 2002a]. At low B_{cr}/B_c values, the corresponding M_{rs}/M_s values are in excess of 0.5, which demonstrates the magnetocrystalline anisotropy of greigite [*Roberts*, 1995; *Roberts et al.*, 2011]. The different trend lines for SD + SP mixtures of magnetite compared to greigite reflect the difference between magnetic particle systems with uniaxial and cubic anisotropy. The calculated trend line for the Crostolo River samples is a smooth curve through the data points and the ensemble of bootstrap trend lines has a consistent structure, which indicates that the analysis has not been unduly influenced by the presence of outliers. Such a result is indicative of a binary mixing system.

[29] As with all regression techniques, our proposed method quantifies the best fit through the data but it does not explain the underlying cause of the relationship. While the line in Figure 3 is statistically the best fit to the data (under the assumption of linear binary mixing), it would be difficult to ascribe the trend to a SD + SP mixing system rather than to a SD + MD system without additional information such as the theoretical mixing lines of *Dunlop* [2002a]. Alternative information could take the form of complementary experimental evidence, or comparisons to empirical studies, which is essential if the nature of the mixing system is to be defined fully. In the present example, greigite is well known to occur within a SD + SP envelope [*Rowan and Roberts*, 2006] and a detailed global data compilation supports this interpretation [*Roberts et al.*, 2011]. Furthermore, the trend line identified in Figure 3 lies well away from empirically determined SD + MD mixing lines for greigite [*Roberts et al.*, 2011]. The small offset of the Crostolo River samples, and hence the resulting best fit line, from the SD + SP greigite mixing system suggests a minor rock magnetic difference between the Crostolo River samples and the global compilation represented in the power law trend line of *Roberts et al.* [2011].

5.2. North Pacific Ocean

[30] A rock magnetic investigation of middle and upper Pleistocene sediments from Ocean Drilling Program (ODP) Hole 883D (Detroit Seamount, North Pacific Ocean) demonstrated that the magnetic mineral assemblage of the clay-rich sediments is dominated by magnetite with relatively uniform grain size [*Roberts et al.*, 1995b]. This limited variability in magnetic grain size was demonstrated using hysteresis ratios, which are restricted to a narrow zone in the PSD field (Figure 4a), a pattern that is consistent with sediment transport and sorting over long distances. A single outlier in the analyzed data set has a coarser magnetite grain size and corresponds to a tephra layer [*Roberts et al.*, 1995b]. As a first step this outlying sample was removed from the analysis and the best fit line through the hysteresis data and 1000 bootstrap iterations were calculated (Figure 4b). The best fit line describes a path through a narrow zone of the PSD field and explains ~70% of the data variance. The bootstrap results form a relatively wide envelope around the best fit line, however, this is not surprising given the scatter of the data. The best fit line lies slightly to the right of the magnetite SD + MD mixing line calculated by *Dunlop* [2002a] based on the data of *Parry* [1980, 1982] and is outside the region expected for SD + SP mixing. Such an offset from SD + MD mixing can be indicative of the presence of PSD grains [*Dunlop*, 2002b], which supports the conclusions of *Roberts et al.* [1995b].

[31] To test the influence of the tephra layer, the analysis was repeated on the full data set with classical and robust

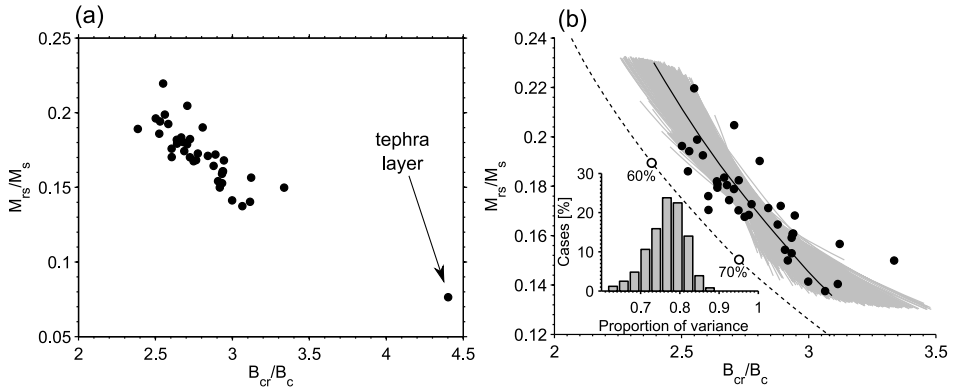

Figure 4. (a) Day plot representation of hysteresis data from the ODP Hole 883D [*Roberts et al.*, 1995b]. Clustering of the data suggests variability across a narrow range of grain sizes. A single coarser-grained sample, from a tephra layer, is outlying with respect to the main body of data. (b) The best fit trend line (black line) and bootstrap trend lines (gray lines) for the Hole 883D samples (black symbols, n = 41) with the tephra layer removed. The dashed line represents the SD + MD magnetite mixing line calculated by *Dunlop* [2002a] based on the data of *Parry* [1980, 1982]. Values quoted next to the open symbols on the SD + MD mixing line indicate the relative amount of MD material. The inset contains the distribution of the bootstrap lines' proportional variances.

forms of eigenvector analysis (Figure 5). While the classical (nonrobust) best fit line is drawn toward the outlying tephra sample, the robust result is in close agreement with the classical best fit line when the tephra sample is removed from the analysis.

[32] The results from this example demonstrate two important points. First, there is an ambiguity associated with clusters of points positioned in a limited region of the Day plot. Such cases may result from binary mixing systems with only small changes in the relative proportions of end-members, or alternatively, from a series of magnetic mineral assemblages with slightly different grain sizes that are not a product of a persistent mixing system. This means that best fit lines should be treated with caution when a collection of samples is limited to a narrow grain size range. Second, as with other least squares techniques, it is essential to consider the presence of outliers. We have demonstrated, however, that the influence of outliers can be reduced using existing robust approaches [*Hawkins et al.*, 2001; *Croux et al.*, 2007].

5.3. Butte Valley, Northern California

[33] The final example is taken from an analysis of Plio-Pleistocene lake sediments from Butte Valley, northern California [*Roberts et al.*, 1996]. Hysteresis loops are available throughout the studied 102 m core. The detrital magnetic mineral assemblage is dominated by titano-magnetite derived from the basaltic bedrock in the lake catchment. Additional analyses (X-ray diffraction and low-temperature measurements on magnetic mineral extracts) also identified the presence of hematite and possibly maghemite within the detrital sediment component. Authigenic greigite was detected in a number of horizons throughout the core. Within the Day plot, the Butte Valley samples have a typical diagonal trend across the diagram, which becomes more scattered toward higher B_{cr}/B_c values (Figure 6). Calculation of the best fit mixing line and associated bootstrap iterations reveals a complex pattern that does not appear to describe the general data pattern and has a form that is not compatible with the known behavior of binary mixtures within natural magnetic mineral assemblages [*Tauxe et al.*, 1996; *Dunlop*, 2002a].

[34] Although there is some scatter in the bootstrap trend lines, reevaluation of the best fit binary mixing model using robust analysis has little influence on the final result (not shown). This indicates that the form of the curve does not result from a small number of outliers. On this evidence, the

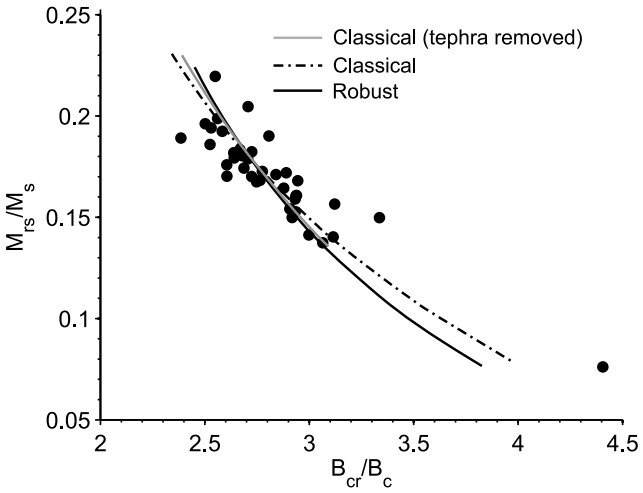

Figure 5. Demonstration of the influence of the outlying tephra sample in the ODP Hole 883D hysteresis data set on the best fit line. In the case of classical least squares analysis, the calculated best fit line (dot-dashed line) is unduly influenced by the outlying point, which pulls the line toward larger values of B_{cr}/B_c in the bottom part of the diagram. If a robust analysis is employed, the influence of the outlier is reduced and the best fit line (black) is in good agreement with the result obtained when the tephra layer is removed from the analysis (gray line).

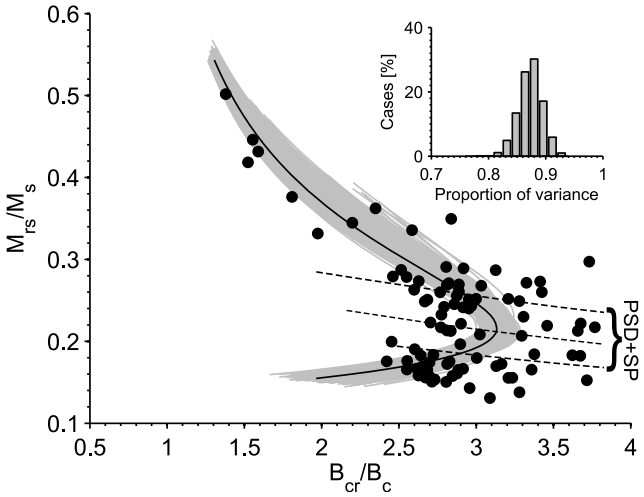

Figure 6. Best fit trend line (black line) and bootstrap trend lines (gray lines) for data from Plio-Pleistocene lake sediments recovered in a core from Butte Valley, northern California [*Roberts et al.*, 1996] (black symbols, n = 91). The suite of PSD + SP mixing lines given by *Dunlop* [2002b] is shown as a collection of dashed lines. In the Day plot the trend line does not provide a good fit to the data and has a form that is not typical of binary mixing systems, which suggests that the sediments contain a more complex magnetic mineral assemblage with at least three magnetic components. The inset is a plot of the distribution of the bootstrap lines' proportional variances.

Butte Valley sediments appear to have a complex magnetic mineral assemblage that cannot be explained by a simple binary mixing model. This interpretation is consistent with conclusions from more detailed rock magnetic studies [*Roberts et al.*, 1996], which demonstrated that the magnetic mineralogy of the Butte Valley samples is controlled by a higher-order mixing scheme. This result demonstrates that best fit binary mixing lines have an important role to play in the identification of higher-order mixing systems that cannot be approximated by two end-members.

[35] Finally, it can be noted that the main body of the data coincides with the PSD + SP mixing lines of *Dunlop* [2002b] (Figure 6). This coincidence could lead to a spurious interpretation of the sediment magnetic mineralogy as being a two-part composition composed of PSD and SP grains. This reinforces the point that the Day plot is a nonunique space and that coincidence of data points in a Day plot with theoretical mixing lines does not provide a sufficient basis to assign a composition or to identify a binary mixing scheme for the data in question. Instead trends though hysteresis data are required to identify binary mixing and in the case of the Butte Valley hysteresis data the best fit line indicates that a binary mixing scheme is not viable.

6. Conclusions

[36] Under an assumption of linear mixing, we have developed a method with which best fit lines can be evaluated through the Day plot for data originating from binary magnetic mineral mixtures. This method can be used to quantify trends in hysteresis data and can help to identify binary mixing systems. While the fitting method can be used to describe the underlying relationship in a data set, more information is required to define the end-members of the mixing scheme. This information could come from the M_{rs}/M_s and B_{cr}/B_c data, however, the nonunique nature of the Day plot [*Tauxe et al.*, 1996] means that independent magnetic and other diagnostic measurements ought to be used to identify the magnetic end-members.

[37] The proposed approach has been demonstrated using geological data sets that evidently originate from binary and more complex mixing systems. Additional work is required to provide a statistical test with which binary mixtures can be identified. However, indicative statistics such as the proportion of the variance explained by linear binary mixing and ensembles of bootstrap-based best fit lines provide a useful guide to model selection. Analysis methods for hysteresis data from magnetic mineral assemblages that contain three or more components are treated in a separate paper (Heslop and Roberts, submitted manuscript, 2011).

[38] **Acknowledgments.** We thank two reviewers and the associate editor for their constructive comments, which helped to improve the final manuscript. This work was supported by the Australian Research Council (grant DP110105419).

References

Carter-Stiglitz, B., B. Moskowitz, and M. Jackson (2001), Unmixing magnetic assemblages and the magnetic behavior of bimodal mixtures, *J. Geophys. Res.*, *106*, 26,397–26,411, doi:10.1029/2001JB000417.

Channell, J. E. T., and C. McCabe (1994), Comparison of magnetic hysteresis parameters of unremagnetized and remagnetized limestones, *J. Geophys. Res.*, *99*, 4613–4623.

Croux, C., P. Filzmoser, and M. Oliveira (2007), Algorithms for projection-pursuit robust principal component analysis, *Chemom. Intell. Lab. Syst.*, *87*, 218–225.

Day, R., M. Fuller, and V. A. Schmidt (1977), Hysteresis properties of titanomagnetites: Grain-size and compositional dependence, *Phys. Earth Planet. Inter.*, *13*, 260–267, doi:10.1016/0031-9201(77)90108-X.

Dunlop, D. J. (2002a), Theory and application of the Day plot (M_{rs}/M_s versus H_{cr}/H_c): 1. Theoretical curves and tests using titanomagnetite data, *J. Geophys. Res.*, *107*(B3), 2056, doi:10.1029/2001JB000486.

Dunlop, D. J. (2002b), Theory and application of the Day plot (M_{rs}/M_s versus H_{cr}/H_c): 2. Application to data for rocks, sediments, and soils, *J. Geophys. Res.*, *107*(B3), 2057, doi:10.1029/2001JB000487.

Dunlop, D. J., and B. Carter-Stiglitz (2006), Day plots of mixtures of superparamagnetic, single-domain, pseudosingle-domain, and multidomain magnetites, *J. Geophys. Res.*, *111*, B12S09, doi:10.1029/2006JB004499.

Efron, B., and R. J. Tibshirani (1993), *An Introduction to the Bootstrap*, Chapman and Hall, New York.

Ehrlich, R., and W. E. Full (1987), Sorting out geology—Unmixing mixtures, in *Use and Abuse of Statistical Methods in the Earth Sciences*, *Stud. Math. Geol.*, vol. 1, edited by W. B. Size, pp. 33–46, Oxford Univ. Press, New York.

Gee, J., and D. V. Kent (1995), Magnetic hysteresis in young mid-ocean ridge basalts: Dominant cubic anisotropy?, *Geophys. Res. Lett.*, *22*, 551–554.

Hawkins, D. M., L. Liu, and S. S. Young (2001), Robust singular value decomposition, *Tech. Rep. 122*, 13 pp., Natl. Inst. of Statist. Sci., Research Triangle Park, N. C.

Heslop, D. (2005), A Monte Carlo investigation of the representation of thermally activated single-domain particles within the Day plot, *Stud. Geophys. Geod.*, *49*, 163–176, doi:10.1007/s11200-005-0003-7.

Jackson, M. (1990), Diagenetic sources of stable remanence in remagnetized Paleozoic cratonic carbonates: A rock magnetic study, *J. Geophys. Res.*, *95*, 2753–2761.

Jackson, M., and P. Solheid (2010), On the quantitative analysis and evaluation of magnetic hysteresis data, *Geochem. Geophys. Geosyst.*, *11*, Q04Z15, doi:10.1029/2009GC002932.

Jolliffe, I. T. (2002), *Principal Component Analysis*, 2nd ed., Springer, New York.

Lanci, L., and D. V. Kent (2003), Introduction of thermal activation in forward modeling of hysteresis loops for single-domain magnetic particles

and implications for the interpretation of the Day diagram, *J. Geophys. Res.*, *108*(B3), 2142, doi:10.1029/2001JB000944.

Lascu, I., S. K. Banerjee, and T. S. Berquó (2010), Quantifying the concentration of ferrimagnetic particles in sediments using rock magnetic methods, *Geochem. Geophys. Geosyst.*, *11*, Q08Z19, doi:10.1029/2010GC003182.

Lees, J. A. (1997), Mineral magnetic properties of mixtures of environmental and synthetic materials: Linear additivity and interaction effects, *Geophys. J. Int.*, *131*, 335–346, doi:10.1111/j.1365-246X.1997.tb01226.x.

Muxworthy, A. R., W. Williams, and D. Virdee (2003), Effect of magnetostatic interactions on the hysteresis parameters of single-domain and pseudo-single-domain grains, *J. Geophys. Res.*, *108*(B11), 2517, doi:10.1029/2003JB002588.

Parry, L. G. (1980), Shape-related factors in the magnetization of immobilized magnetite particles, *Phys. Earth Planet. Inter.*, *22*, 144–154, doi:10.1016/0031-9201(80)90055-2.

Parry, L. G. (1982), Magnetization of immobilized particle dispersions with two distinct particle sizes, *Phys. Earth Planet. Inter.*, *28*, 230–241, doi:10.1016/0031-9201(82)90004-8.

Pike, C. R., A. P. Roberts, and K. L. Verosub (1999), Characterizing interactions in fine magnetic particle systems using first order reversal curves, *J. Appl. Phys.*, *85*, 6660–6667, doi:10.1063/1.370176.

Roberts, A. P. (1995), Magnetic characteristics of sedimentary greigite (Fe_3S_4), *Earth Planet. Sci. Lett.*, *134*, 227–236, doi:10.1016/0012-821X(95)00131-U.

Roberts, A. P., Y. Cui, and K. L. Verosub (1995a), Wasp-waisted hysteresis loops: Mineral magnetic characteristics and discrimination of components in mixed magnetic systems, *J. Geophys. Res.*, *100*, 17,909–17,924, doi:10.1029/95JB00672.

Roberts, A. P., K. L. Versosub, R. J. Weeks, B. Lehman, and C. Laj (1995b), Mineral magnetic properties of middle and upper Pleistocene sediments at sites 883, 884, and 887, North Pacific Ocean, *Proc. Ocean Drill. Program Sci. Results*, *145*, 483–490.

Roberts, A. P., R. L. Reynolds, K. L. Verosub, and D. P. Adam (1996), Environmental magnetic implications of greigite (Fe_3S_4) formation in a 3 m.y. lake sediment record from Butte Valley, northern California, *Geophys. Res. Lett.*, *23*, 2859–2862.

Roberts, A. P., C. R. Pike, and K. L. Verosub (2000), First-order reversal curve diagrams: A new tool for characterizing the magnetic properties of natural samples, *J. Geophys. Res.*, *105*, 28,461–28,475, doi:10.1029/2000JB900326.

Roberts, A. P., W. T. Jiang, F. Florindo, C. S. Horng, and C. Laj (2005), Assessing the timing of greigite formation and the reliability of the Upper Olduvai polarity transition record from the Crostolo River, Italy, *Geophys. Res. Lett.*, *32*, L05307, doi:10.1029/2004GL022137.

Roberts, A. P., L. Chang, C. J. Rowan, C.-S. Horng, and F. Florindo (2011), Magnetic characteristics of sedimentary greigite (Fe_3S_4): An update, *Rev. Geophys.*, *49*, RG1002, doi:10.1029/2010RG000336.

Rousseeuw, P. J., and B. C. van Zomeren (1990), Unmasking multivariate outliers and leverage points, *J. Am. Stat. Assoc.*, *85*, 633–651.

Rowan, C. J., and A. P. Roberts (2006), Magnetite dissolution, diachronous greigite formation, and magnetizations arising from pyrite oxidation: Unravelling complex magnetizations in Neogene marine sediments from New Zealand, *Earth Planet. Sci. Lett.*, *241*, 119–137, doi:10.1016/j.epsl.2005.10.017.

Sprowl, D. R. (1990), Numerical estimation of interactive effects in single-domain magnetite, *Geophys. Res. Lett.*, *17*, 2009–2012.

Suk, D., and S. L. Halgedahl (1996), Hysteresis properties of magnetic spherules and whole rock specimens from some Paleozoic platform carbonate rocks, *J. Geophys. Res.*, *101*, 25,053–25,075.

Tauxe, L., T. A. T. Mullender, and T. Pick (1996), Potbellies, wasp-waists, and superparamagnetism in magnetic hysteresis, *J. Geophys. Res.*, *101*, 571–583, doi:10.1029/95JB03041.

Tric, E., C. Laj, C. Jehanno, J.-P. Valet, C. Kissel, A. Mazaud, and S. Iaccarino (1991), High-resolution record of the Upper Olduvai transition from Po Valley (Italy) sediments: Support for dipolar transition geometry?, *Phys. Earth Planet. Inter.*, *65*, 319–336, doi:10.1016/0031-9201(91)90138-8.

D. Heslop and A. P. Roberts, Research School of Earth Sciences, Australian National University, Bldg. 61, Mills Rd., Canberra, ACT 0200, Australia. (david.heslop@anu.edu.au; andrew.roberts@anu.edu.au)